The Canadian Mineralogist
Vol. 31, pp. 583-595 (1993)

THE CRYSTAL CHEMISTRY OF STAUROLITE. II. ORDER – DISORDER AND THE MONOCLINIC → ORTHORHOMBIC PHASE TRANSITION

FRANK C. HAWTHORNE[1], LUCIANO UNGARETTI, ROBERTA OBERTI, FRANCA CAUCIA AND ATHOS CALLEGARI

CNR Centro di Studio per la Cristallochimica e la Cristallografia, via Bassi 4, I-27100 Pavia, Italy

ABSTRACT

Crystal structures of staurolite refined in the space group *C2/m* show a range of angles from 90 to 90.45°. Many reports of cell dimensions with β = 90° probably reflect restrictions of the experimental method used rather than the character of the material. The staurolite structure is pseudo-orthorhombic, and the displacements of all (except one of) the atomic positions from their ideal values for the orthorhombic (*Ccmm*) case are continuous linear functions of the β angle. In addition, the Al – □, (Fe,Mg) – □ and (Fe,Zn...) – □ order over the *M*(3*A*) – *M*(3*B*), *M*(4*A*) – *M*(4*B*) and *T*(2) subsites, respectively, are linear functions of β. These relationships are all compatible with a continuous second-order phase-transition between an orthorhombic *Ccmm* structure and a monoclinic *C2/m* structure. However, the *x* coordinate of the O(4) anion is constant with varying β, and significantly (~ 0.15 Å) displaced from its ideal position in the orthorhombic structure. Thus there may be a small amount of first-order character to the transition; alternatively, it could be completely second-order, with all displacements except for *x* O(4) quenchable to room temperature. Thus staurolite is an order–disorder series between a completely disordered orthorhombic end-member [*Ccmm*, β = 90°, *M*(3*A*) = *M*(3*B*) = 0.5 Al + 0.5 □] and a fully ordered monoclinic end-member [space group *C2/m*, β = 90.64°, *M*(3*A*) = Al, *M*(3*B*) = □]. *C2/m* is an isotropy subgroup of *Ccmm*. Examination of all atomic displacements and patterns of cation order that transform as the active irreducible representation associated with the transition suggests that the Al – □ ordering over the *M*(3*A*) – *M*(3*B*) sites is the primary order-parameter driving the transition.

Keywords: staurolite, order–disorder, phase transition.

SOMMAIRE

Les ébauches de la structure cristalline de la staurotide affinées dans le groupe spatial *C2/m* montrent un variabilité dans l'angle β de 90 à 90.45°. Plusieurs exemples de maille ayant un angle β de 90° résultent probablement des restrictions implicites dans l'approche expérimentale plutôt que d'une propriété intrinsèque d'un échantillon. La structure de la staurotide est pseudo-orthorhombique, et les déplacements impliquant toutes les positions atomiques (sauf une) de leurs positions dans la structure idéale orthorhombique (*Ccmm*) sont des fonctions linéaires de l'angle β. De plus, les degrés d'ordre impliquant Al – □, (Fe,Mg) – □, et (Fe,Zn...) – □ impliquant les sous-positions *M*(3*A*) – *M*(3*B*), *M*(4*A*) – *M*(4*B*), et *T*(2), respectivement, sont aussi des fonctions linéaires de β. Ces relations sont toutes compatibles avec une transition continue de deuxième ordre entre une structure orthorhombique *Ccmm* et une structure monoclinique *C2/m*. Toutefois, la coordonnée *x* de l'atome O(4) est constante malgré les variations dans l'angle β, et déplacée de façon significative (0.15 Å) par rapport à sa valeur dans la structure orthorhombique idéale. Il pourrait donc y avoir une légère contribution d'un caractère de premier ordre à cette transition. Toutefois, la transition pourrait aussi avoir un caractère entièrement de deuxième ordre, et exprimer la propriété que tous les déplacements à l'exception de celui impliquant O(4) sont conservés lors du refroidissement à la température ambiante. C'est donc dire que la staurotide témoigne d'un phénomène ordre – désordre entre un pôle complètement désordonné, orthorhombique [groupe spatial *Ccmm*, β = 90°, *M*(3*A*) = *M*(3*B*) = 0.5 Al + 0.5 □] et un pôle complètement ordonné, monoclinique [*C2/m*, β = 90.64°, *M*(3*A*) = Al, *M*(3*B*) = □]. Le groupe spatial *C2/m* est un sous-groupe isotrope de *Ccmm*. Une étude de tous les déplacements atomiques et de la mise en ordre des cations qui se déplacent, dans l'expression irréductible active de la transition, fait penser que c'est la mise en ordre de Al et des lacunes sur les sites *M*(3*A*) et *M*(3*B*) qui est le phénoménologiquement responsable de la transition.

(Traduit par la Rédaction)

Mots-clés: staurotide, ordre – désordre, transition de phase.

---

[1] Permanent address: Department of Geological Sciences, University of Manitoba, Winnipeg, Manitoba R3T 2N2.

Introduction

The crystal structure of staurolite was originally determined by Náray-Szabó (1929) in the orthorhombic space-group *Ccmm*. Subsequently, Hurst *et al.* (1956) proposed that staurolite is monoclinic *C2/m* with only orthorhombic pseudo-symmetry, and most of the subsequent structural studies (Smith 1968, Tagai & Joswig 1985, Bringhurst & Griffen 1986, Ståhl *et al.* 1988, Alexander 1989) have supported this view. Except for the staurolite of Alexander (1989), all the other samples reported in the literature have $\beta = 90°$. The staurolite samples examined by Hawthorne *et al.* (1993a) show a considerable range of β values, from 90.00 to 90.45°, and the large number of samples deviating significantly from $\beta = 90°$ suggests that such deviations are the rule rather than the exception for staurolite. To characterize deviations from $\beta = 90°$, refinement of cell dimensions by the powder method requires resolution and consistent indexing of $(h,k,\pm l)$ pairs of reflections; for values of β close to 90°, this is not feasible, and cell dimensions of staurolite measured by powder diffraction (except perhaps for the Rietveld method) will all have $\beta = 90°$. This is not the case for cell dimensions determined by single-crystal diffractometry, as the reflections (h,k,l) and $(h,k,\bar{l})$ are well resolved in three dimensions, and both resolution and consistency of indexing are easy to obtain. This suggests that the generally reported result of $\beta = 90°$ is predominantly due to restrictions of the experimental method used. In support of this argument, we find that many structural parameters correlate with the β angle (see below), and the same parameters from previous structural studies suggest that the β angle commonly must deviate significantly from 90° in the crystals examined. All quantitative arguments used here will generally be based on the refined structures of Hawthorne *et al.* (1993a); for ease of expression in the following arguments, this source of data will not be referenced further.

Does Orthorhombic Staurolite Exist?

Some of the refined samples of staurolite have β equal to 90° (in the space group *C2/m*), and the question now arises as to whether or not staurolite can truly be orthorhombic. The fact that β is equal to 90° is a necessary but not sufficient condition for orthorhombic symmetry. In order to be orthorhombic, the complete (long-range) structure must obey orthorhombic symmetry. There are two ways in which we can examine this question: (i) directly by analysis of the Laue symmetry of the diffracted X-ray intensities, and (ii) by consideration of the possible orthorhombic nature of the refined structures.

Laue Symmetry

Orthorhombic staurolite would have Laue symmetry *mmm*, whereas monoclinic staurolite has Laue symmetry *2/m*. The principal differences between these two groups are the mirror planes perpendicular to *a* and *c*, present in *mmm* but absent in *2/m*. Thus the differences in symmetry between these two Laue groups will be apparent by comparison of diffracted intensities of the form *hkl* and $\bar{h}kl$ or *hkl* and $hk\bar{l}$ (such pairs are symmetrically distinct in *2/m* but equivalent in *mmm*). Inspection of the diffracted intensities shows that the reflections {201} and {$\bar{2}$01} have a wide variation in relative intensities with varying β angle, and can serve to examine the Laue symmetry. The absolute magnitudes of the structure factors depend on many factors unconnected with the question of Laue symmetry; the magnitudes of the structure factors examined must be normalized in order to remove such effects. Here we will use the function *L*, where

$$L = (|F_{\bar{2}01}| - |F_{201}|) / (|F_{\bar{2}01}| + |F_{201}|) \quad (1)$$

If $|F_{\bar{2}01}|$ is equal to $|F_{201}|$, *L* is 0, and Laue symmetry *mmm* is obeyed. Where $|F_{\bar{2}01}|$ is greater than $|F_{201}|$, *L* is non-zero, and *mmm* symmetry is broken; note that $|F_{\bar{2}01}|$ less than $|F_{201}|$ is not observed in these crystals (with one weak exception). Figure 1 shows the variation of L with β for 42 crystals of staurolite.

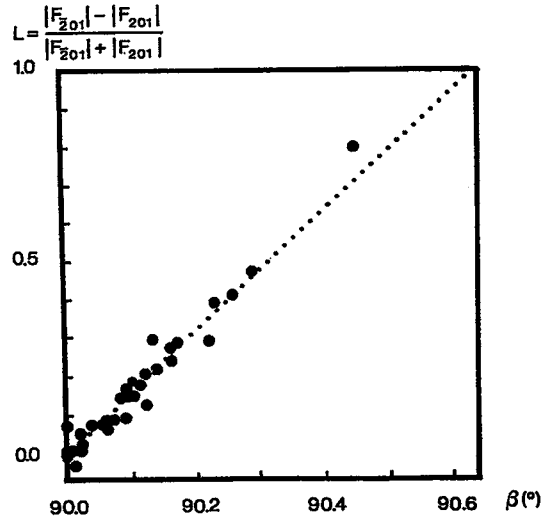

FIG. 1. Variation in *L* [=($|F_{\bar{2}01}| - |F_{201}|$) / ($|F_{\bar{2}01}| + |F_{201}|$)] as a function of β angle for staurolite crystals refined in the space group *C2/m*. The line is not a least-squares line, but is drawn through $Q = 0$, $\beta = 90°$ and $Q = 1$, $\beta = 90.64°$ (see text and Fig. 3), the latter being the maximum value of β for the fully ordered monoclinic end-member.

rolite; there is a well-developed linear relationship that passes through the point $\beta = 90°$, $L = 0$, and seems to indicate a continuous variation in L with varying β angle. It is notable that there are several data that occur at $\beta = 90°$, $L = 0$, indicating that this specific set of reflections obeys *mmm* Laue symmetry for these crystals.

Space-Group Symmetry

If an orthorhombic structure is refined in space-group symmetry *C2/m*, the constraints of monoclinic symmetry allow it to refine to an orthorhombic arrangement. In this way, the symmetry of the diffraction pattern can be examined *in toto*, with the added advantage that the important parameters involved in the differences in symmetry can be identified. There is no change of origin involved in the transition from *Ccmm* to *C2/m*, and the atomic coordinates will correspond in each symmetry without a change of origin or orientation of the unit cell; a comparison of the positions is shown in Table 1. The changes in parameters will be examined in detail here, both to characterize the change in space group and later to develop a microscopic model for the phase transition.

Order–disorder at M(3A) and M(3B)

In a *Ccmm* structure of staurolite, adjacent octahedra would be symmetrically equivalent [*i.e.*, $M(3A) = M(3B)$], whereas in the *C2/m* staurolite structure, adjacent octahedra are distinct (*i.e.*, $M(3A) \neq M(3B)$] (Fig. 2a). In the *C2/m* structure refinement of Náray-Szabó & Sasvári (1958), all available Al was assigned to the $M(3A)$ site; thus $M(3A)$ was considered as fully occupied, and $M(3B)$ was considered empty. Conversely, in the *Ccmm* structure refinement of Hanisch (1966), both $M(3A)$ and $M(3B)$ were considered as half-occupied. In his classic structural study of staurolite, Smith (1968) showed that (Al+Fe) is partially ordered between the $M(3A)$ and $M(3B)$ sites in the space group *C2/m*. Similar partial ordering over these sites has since been observed by Tagai & Joswig (1985), Bringhurst & Griffen (1986), Ståhl *et al.* (1988) and Alexander (1989), with the scattering power and assigned populations at $M(3A)$ always exceeding those at $M(3B)$.

The difference in occupancy at the $M(3)$ sites may be represented in a similar fashion to the diffracted intensities examined above. If $X_{M(3A)}$ represents the occupancy of the $M(3A)$ site, then the order parameter $Q_{M(3)}$ is defined as follows:

$$Q_{M(3)} = (X_{M(3A)} - X_{M(3B)})/(X_{M(3A)} + X_{M(3B)}) \quad (2)$$

As shown in Figure 3, $Q_{M(3)}$ is a function of the angle β. There is an extremely well-developed correlation, showing that the variation in β does indeed reflect a direct structural deviation from orthorhombic symmetry. This variation is particularly interesting, as it allows us to fix the maximum possible value for the difference in site occupancies. When $Q_{M(3)} = 1$, $M(3A)$ is completely occupied, and $M(3B)$ is completely vacant. This situation represents a maximum possible deviation from equivalence of the two sites in the orthorhombic case, and suggests a maximum limit for the β angle. As can be seen in Figure 3, the maximum value of β is 90.64°, coinciding with complete Al – □ ordering at $M(3A)$ and $M(3B)$, respectively.

It is particularly notable that this order–disorder *versus* β relationship seems to be compositionally independent. The trend of Figure 3 includes all compositional varieties of staurolite examined here: Fe-rich, Mg-rich, Zn-rich and Li-rich staurolites; they all follow the same relationship. This presumably reflects the fact that $M(3A)$ and $M(3B)$ are dominantly to completely occupied by Al and □, with little occupancy by any other species. On the other hand, it is surprising that the relationship is not perturbed by compositional variations at other sites in staurolite, particularly the $T(2)$ site. Of particular interest in this regard is the Zn-rich staurolite 117189. Cell dimensions were measured on 14 crystals from the powdered separate of this sample, and these show the complete observed range of β from 90.00 to 90.45°, greater than the total range in β shown by all the other samples of staurolite examined here. Structures were refined for four of these crystals covering the total variation. Both the compositions derived from the refined structures and

TABLE 1. THE COORDINATE TRANSFORMATIONS IN THE *Ccmm* → *C2/m* TRANSITION IN STAUROLITE

Orthorhombic						Monoclinic				
O(1)	8f	x	0	z	<----	O(1A)	4i	x	0	z
					<----	O(1B)	4i	x	0	z
O(2)	16h	x	y	z	<----	O(2A)	8j	x	y	z
					<----	O(2B)	8j	x	y	z
O(3)	8g	x	y	¼	-----	O(3)	8j	x	y	z
O(4)	8d	0	¼	¼	-----	O(4)	8j	x	y	z
O(5)	8g	x	y	¼	-----	O(5)	8j	x	y	z
T(1)	8g	x	y	¼	-----	T(1)	8j	x	y	z
T(2)	4c	x	0	¼	-----	T(2)	4i	x	0	z
M(1)	8f	½	y	0	-----	M(1A)	4g	½	y	0
					-----	M(1B)	4g	½	y	0
M(2)	8g	x	y	¼	-----	M(2)	8j	x	y	z
M(3)	4a	0	0	0	<----	M(3A)	2a	0	0	0
					<----	M(3B)	2c	0	0	½
M(4)	4b	½	0	0	<----	M(4A)	2b	½	0	0
					<----	M(4B)	2d	½	0	½

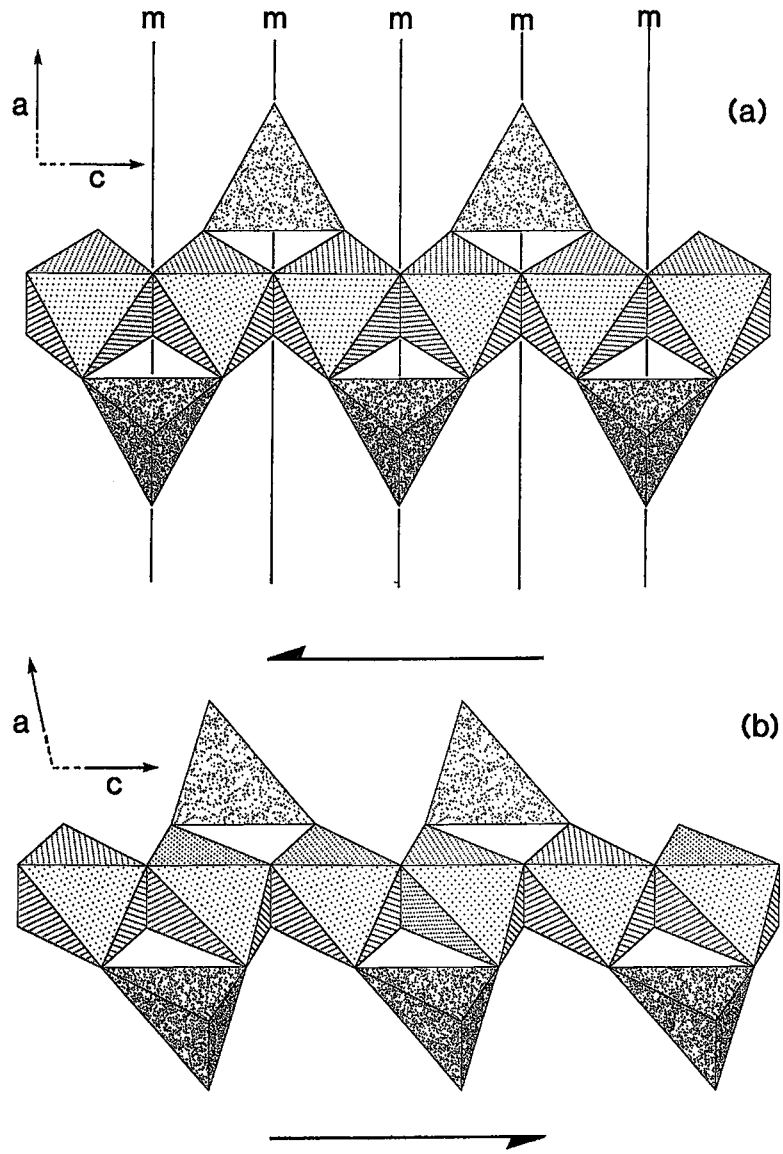

FIG. 2. The $M(3A)$, $M(3B)$ (periodic dot pattern) and $T(2)$ (random dot pattern) polyhedra in staurolite; adjacent $M(3A)$ and $M(3B)$ octahedra share edges to form a simple *trans* edge-sharing chain that is decorated by staggered $T(2)$ tetrahedra; (a) the arrangement with *Ccmm* symmetry, in which adjacent octahedra are related by mirrors perpendicular to the *c* axis; (b) the arrangement with *C2/m* symmetry (very exaggerated, with $\beta \approx 110°$), in which adjacent octahedra are symmetrically distinct; the orthorhombic → monoclinic distortion is shown as a shear along the *c* axis.

the compositions measured by electron microprobe on those same crystals showed no significant variation with β; the only major difference from structure to structure was found to be the relative degree of Al – □ ordering over $M(3A)$ and $M(3B)$.

The geometry of the M(3A) and M(3B) octahedra

Another very obvious indicator of the monoclinic character of the staurolite structure is the nature of the $M(3A)$ and $M(3B)$ polyhedra, as has been suggested by

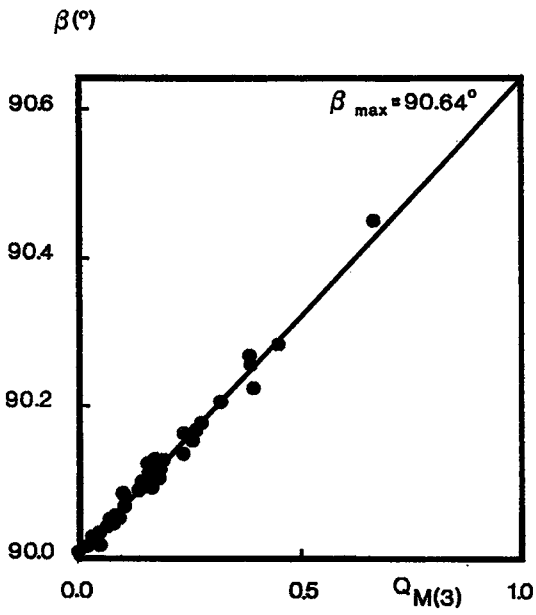

FIG. 3. Variation in $Q_{M(3)}$ [=$(X_{M(3A)} - X_{M(3B)})/(X_{M(3A)} + X_{M(3B)})$ occupancies] as a function of β angle in staurolite crystals refined in the space group *C2/m*. The line is a least-squares fit to the data, and intersects $Q_{M(3)} = 1$ at β = 90.64°.

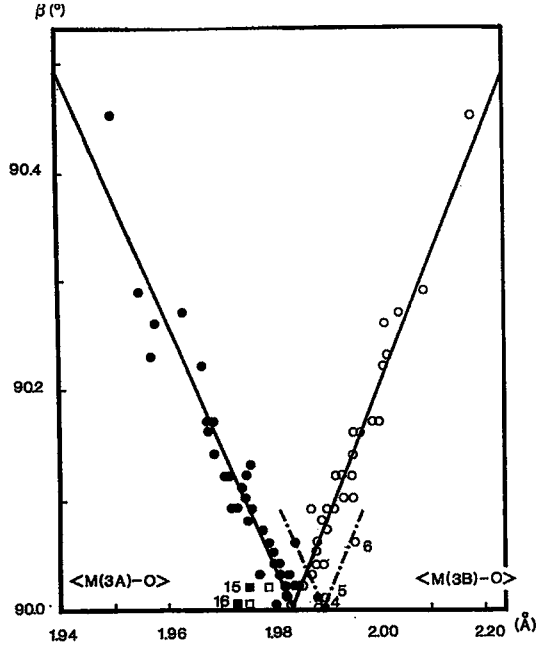

FIG. 4. Variation in mean bond-lengths of the *M*(3*A*) and *M*(3*B*) octahedra as a function of β angle in staurolite crystals refined in the space group *C2/m*; filled circles represent *M*(3*A*), hollow circles represent *M*(3*B*). The least-squares lines through each arm of the graph intersect at β = 90°. The parallel dashed trends refer to Mg-rich staurolite; the squares denote Li-rich staurolite.

previous investigators (Smith 1968, Ribbe 1982). The *M*(3*A*) and *M*(3*B*) sites are pseudosymmetrically related by a pseudomirror plane orthogonal to [001] and passing through the shared edge of the *M*(3*A*) – *M*(3*B*) chain (Fig. 2b). As exact identity of the two sites and of their coordination polyhedra must combine with β = 90° for exact symmetry across this pseudomirror plane, it seems reasonable to look for a correlation between lack of symmetry at and about *M*(3*A*) and *M*(3*B*) with deviations of β from 90°; this is done in Figure 4. There is an extremely strong correlation between the sizes of the *M*(3*A*) and *M*(3*B*) octahedra as a function of β (β = 111.5806 – 10.8774 <*M*(3*A*)–O>, *R* = –0.948; β = 65.9388 + 12.1323 <*M*(3*B*)–O>, *R* = 0.975). At β = 90°, the two octahedra are essentially equal in size, the two regression lines intersecting at 1.9835 Å. With increasing β, the sizes of the two octahedra diverge, *M*(3*A*) becoming smaller, and *M*(3*B*) becoming larger. There seems to be some slight perturbation to this trend as a result of differing composition, with Mg- and Li-rich staurolites deviating significantly from the trend for the *M*(3*A*) octahedron (Fig. 4). For Li-rich staurolite S(15–16), both <*M*(3*A*)–O> and <*M*(3*B*)–O> are displaced from the general trend to smaller values. For Mg-rich staurolite S(4–6), a parallel trend is observed (broken line in Fig. 4) displaced to larger values. This observation is consistent with the assignment of small amounts of Mg to *M*(3) in this sample.

Order–disorder at M(4A) and M(4B)

The partly occupied *M*(4*A*) and *M*(4*B*) sites are a very important aspect of staurolite, and proved to be the key in identifying its stoichiometric formula. These sites are both octahedrally coordinated and are symmetrically distinct only in *C2/m* symmetry; they become equivalent in *Ccmm* symmetry. These sites are generally occupied by Fe and Mg (in very Mg-rich samples), and are invariably (in all crystals so far examined) only partly occupied. As with the *M*(3*A*) and *M*(3*B*) sites, their relative occupancies are very variable. Figure 5 shows the variation in relative occupancy [expressed as $Q_{M(4)}$ in the same manner as for the *M*(3*A*) and *M*(3*B*) sites] as a function of β. Again, there is a well-developed linear correlation (although there is considerably more scatter to the data due to the very small occupancies involved in most crystals); a least-squares fit to the data passes through the point

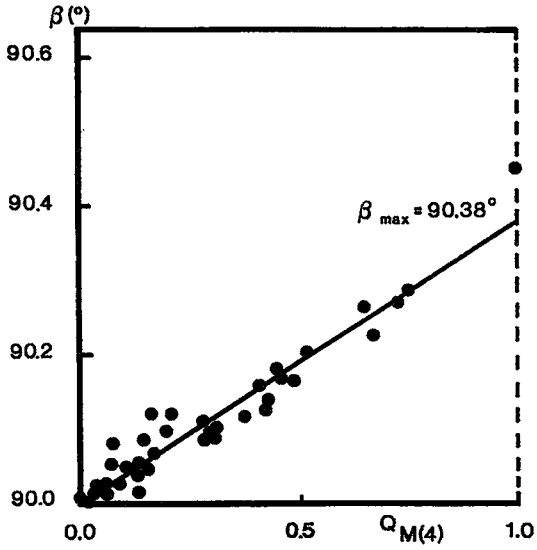

FIG. 5. Variation in $Q_{M(4)}$ [$=(X_{M(4A)} - X_{M(4B)})/(X_{M(4A)} + X_{M(4B)})$ occupancies] as a function of β angle in staurolite crystals refined in the space group *C*2/*m*. The line is a least-squares fit to the data, and intersects $Q_{M(4)} = 1$ at β = 90.38°.

$Q_{M(4)} = 0$, β = 90°. Note the difference between the correlations for $Q_{M(3)}$ and $Q_{M(4)}$: the maximum possible order extrapolates to different values of the β angle (90.64 and 90.38°, respectively); this point will be discussed later.

Pseudo-equivalent atomic positions

In the *C*2/*m* staurolite structure, all atomic positions labeled *A* are pseudo-equivalent to the analogous positions labeled *B*. If the variation in β angle represents deviation from a truly orthorhombic structure, such positions should converge on their ideal "*Ccmm*" positions and occupancies with decreasing β angle, to attain these values at β = 90°. As shown above, the occupancies of the *M*(3) and *M*(4) pairs of sites show this type of behavior. For the other pseudo-equivalent positions, the relevant pairs of coordinates are as follows:

O(1*A*),O(1*B*)	*x*		*z*
O(2*A*),O(2*B*)	*x*	*y*	*z*
M(1*A*),*M*(1*B*)		*y*	

The variations of these parameters are best expressed as the differences between corresponding coordinates, such that the values fall to zero where they become equivalent. These differences as a function of β angle are shown in Figure 6. All differences are monotonic functions of the β angle. Parameters that are pseudo-equivalent in *C*2/*m* symmetry converge and become equal (or equivalent) at β = 90°.

Pseudospecial atomic positions

Many of the atoms in the staurolite structure lie on special positions in the space group *Ccmm*. For some atoms [O(3), O(4), O(5), *T*(1), *T*(2), *M*(2), H(1), H(2)], the transition involves not a splitting of positions but a relaxation of the constraints imposed by *Ccmm* symmetry. The details of this relaxation can be seen in Table 1; the relevant coordinates of these positions are as follows:

O(3), O(5), *T*(1), *T*(2), *M*(2)			*z*
O(4)	*x*	*y*	*z*

The variations in these parameters may be expressed as the differences between their ideal values (for *Ccmm* symmetry) and the observed values. These differences are shown as a function of β angle in Figure 7. In the case of the *T*(2) site, this simple situation is somewhat complicated by the extensive positional disorder that is characteristic of the cations occupying this site, as their separation is too small to derive unique positions and populations. However, we can examine the behavior of the aggregate site indirectly by averaging the *z* coordinates of the three subsites (Fig. 7).

A second-order transition requires that the differences between the two structures go continuously to zero at β = 90°. Most parameters satisfy this condition; there are three exceptions. The *z* parameter of *T*(2) deviates from its ideal value of 1/4 at β = 90° by 0.0005; however, this parameter is actually an aggregate positional parameter, being affected also by the positional disorder over three subsites within the *T*(2) tetrahedron. Thus this small difference from ideal behavior may reflect some degree of residual positional order over the subsites. The other two deviations occur for the *x* and *y* coordinates of the O(4) anion. The *y* coordinate of O(4) shows virtually no significant variation with β, and has a deviation of 0.0006 from its ideal value. The *x* coordinate also does not show much variation with β, but has a much larger deviation, 0.0215, from its ideal value of 0 at β = 0. There are three possibilities for the O(4) anion in an orthorhombic structure: (1) it could occur exactly at the special position 0 1/4 1/4, (2) it could be disordered off this special position, or (3) the symmetry could be lower than *Ccmm*. If (1) were the case, there would be a sudden discontinuous displacement associated with the actual transition. For (2), the disorder in an orthorhombic structure cannot correspond to the positional displacement in the monoclinic structure, as the latter O(4) displacements are ordered. If we propose an orthorhombic symmetry lower than *Ccmm* (*e.g.*, *Cc*2*m*), then *C*2/*m* is no longer an isotropy subgroup of the high-symmetry group, and many of the correspondences shown at β = 90° (Figs. 6, 7) become accidental; this does not seem physically reasonable,

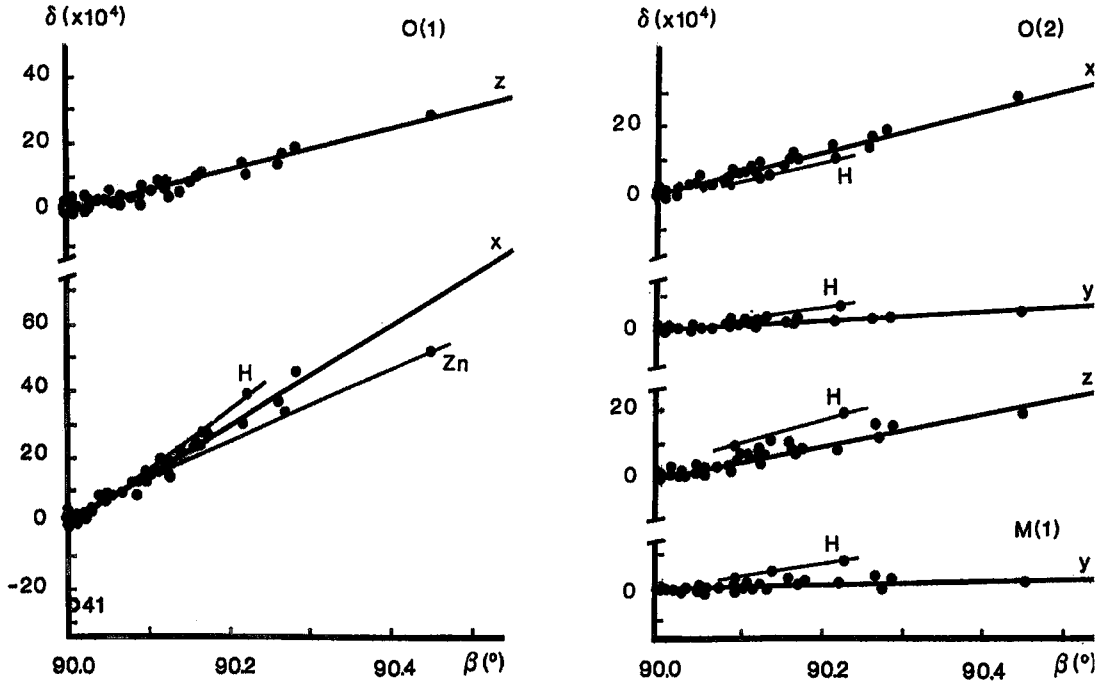

FIG. 6. Variation in free positional parameters, δ [$=(x, y, z)_A - (x, y, z)_B$] $\times 10^4$, for pseudo-equivalent atoms in staurolite crystals with *C2/m* symmetry as a function of β angle; H and Zn refer to separate trends for H-rich and Zn-rich staurolite crystals.

and in the absence of specific evidence to the contrary, we discount this possibility. Consequently, condition (1) or (2) must hold, and there may be discrete displacements at the transition; hence there may be a small amount of first-order character.

Space-group symmetry of staurolite

Most crystals of staurolite are demonstrably monoclinic, with space-group symmetry *C2/m*. However, the detailed data and arguments given above show that some crystals are extremely close to being truly orthorhombic. Although refined with the constraints of *C2/m* space-group symmetry, the structure refinements converged to atomic arrangements with complete *Ccmm* symmetry *except* for a small displacement of the O(4) anion; *thus the room-temperature structure is never truly orthorhombic* (at least in the suite of samples examined here). However, it seems reasonable that with increasing temperature, O(4) will attain its ideal position, and there will be complete *Ccmm* symmetry. There are two possibilities here: (1) the *x* coordinate of O(4) could go continuously to zero with increasing temperature, giving a completely second-order transition, or (2) it could go discontinuously to zero, giving a small amount of first-order character to the transition. Whichever is the case, there is a specific temperature at which the transition occurs. Feasibly this transition temperature is significantly dependent on composition, although we regard this as unlikely, as the behavior of all the order parameters seems fairly independent of composition.

Staurolite as an order–disorder series

Inspection of Figures 3 and 5 shows that we can think of staurolite as an order–disorder series. This is best illustrated for the *M*(3*A*) and *M*(3*B*) sites (Fig. 3), where extensive Al – □ ordering occurs. There is total Al – □ disorder over *M*(3*A*) and *M*(3*B*) at one end of the series [with $\beta = 90°$ and (almost complete) *Ccmm* orthorhombic symmetry] and complete Al – □ order at *M*(3*A*) and *M*(3*B*) at the other end (with $\beta = 90.64°$ and *C2/m* monoclinic symmetry). There is a similar relationship for (Fe,Mg) – □ ordering over the *M*(4*A*) and *M*(4*B*) sites (Fig. 5), but the completely ordered arrangement occurs at a smaller β angle. As β continues to increase past this value (although this is based only on one structure), it seems reasonable to conclude that ordering over *M*(3*A*) and *M*(3*B*) is more important than ordering over *M*(4*A*) and *M*(4*B*) in controlling the deviation from orthorhombic symmetry. This conclu-

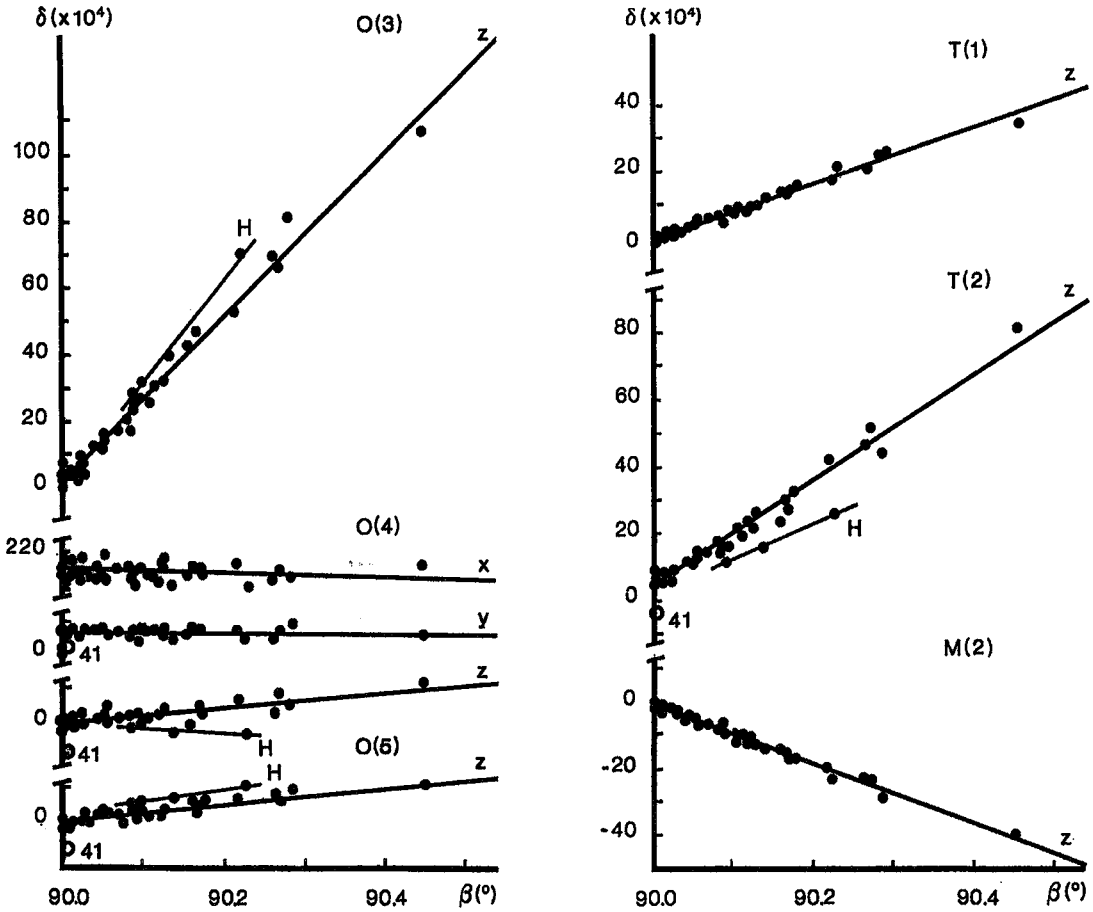

FIG. 7. Variation in symmetry-breaking shifts in positional parameters, $\delta\ [(x, y, z)_m - (x, y, z)_o] \times 10^4$, with β angle for staurolite crystals; m denotes monoclinic, o denotes orthorhombic, and H refers to separate trends for H-rich staurolite crystals.

sion is also in line with the fact that *M*(4*A*) and *M*(4*B*) may be completely vacant for some compositions, and hence cannot be the primary order-parameter for these compositions. In addition, the low *M*(4*A*) and *M*(4*B*) populations for most compositions suggest that ordering of this small number of atoms is unlikely to be energetically more important than the ordering of a much larger number of atoms of higher charge [*i.e.*, Al – □ ordering over *M*(3*A*) and *M*(3*B*)]. There are other parameters that also vary as a function of β angle, and it is possible that one of these is actually more important than Al – □ order over *M*(3*A*) and *M*(3*B*) in controlling the variation in β angle (although we do not consider that this is likely). In this case, the β angle might exceed the value of 90.64° proposed on the basis of Figure 3. However, we will proceed under the assumption that this is not so, and that 90.64° is a maximum possible β value for monoclinic staurolite.

Bond lengths for the fully ordered monoclinic structure

As we know the value of β for complete Al–□ order over *M*(3*A*) and *M*(3*B*), we can calculate the expected mean bond-lengths for the fully ordered structure by extrapolating the linear relationships of Figure 4 to the maximum value of the angle β. This results in <*M*(3*A*) – O> = 1.925 Å for complete Al occupancy, and <*M*(3*B*) – O> = 2.036 Å for zero occupancy. We can derive the radius of the vacancy either by subtraction of the same anion radius from the ideal vacant <*M*(3*B*) – O> distance [r = 2.036 – 1.37 = 0.66 Å] or *via* the difference in the <*M*(3*A*) – O> and <*M*(3*B*) – O> distances in the ordered monoclinic end-member [r = 2.036 – 1.925 + 0.535 = 0.65 Å] (radii from Shannon 1976). Both are compatible with a vacancy radius of ~0.66 Å.

THE *Ccmm* → *C2/m* TRANSITION IN STAUROLITE

As *C2/m* is a subgroup of *Ccmm*, such a transition can be continuous, a possibility that is suggested by the continuous nature of the parameter changes in Figures 1 to 7. Such behavior is conveniently considered within the formalism of the Landau theory of phase transitions. A brief description is given below; more extensive discussions are given by Tolédano & Tolédano (1987) and Kocinski (1983), and applications to minerals by Salje (1985, 1987), Salje *et al.* (1985), Carpenter *et al.* (1990a, b), Ghose *et al.* (1991) and Hatch *et al.* (1990a, b).

Let $p(r)$ be a density function that describes the probability distribution of atomic positions in the crystal. This function is invariant under all symmetry operations of the space group of the crystal. Following Hatch & Griffen (1989), $p(r)$ can be decomposed into a linear combination of basis functions of the physically irreducible representations of the space group:

$$p(r) = \Sigma\Sigma\, \eta_i^{(m)} \varphi_i^{(m)}(r) \qquad (3)$$

where the $\varphi_i^{(m)}$ is the ith basis function of the mth irreducible representation, and $\eta_i^{(m)}$ are the coefficients representing the amplitude of each basis function; $\{\eta_1^{(m)}, \eta_2^{(m)} \ldots \eta_n^{(m)}\}$ is called the *order parameter*, and its number of components, n, is equal to the dimension of the matrices of the mth irreducible representation.

Where there is a continuous phase-transition from a high-symmetry structure to a low-symmetry structure, we may write the density function as

$$p(r) = p(r)_H + \delta p(r) \qquad (4)$$

where the subscript H denotes the high-symmetry phase and $\delta p(r)$ denotes the distortions from that symmetry. This distortion may be written (Hatch *et al.* 1987) as

$$\delta p(r) = \Sigma \eta_i^{(m)} \varphi_i^{(m)}(r) \qquad (5)$$

where $\{\eta_i^{(m)}\}$ is the order parameter that drives the distortion. This is known as the *active representation*, and is that representation of the parent space-group that transforms to the identity representation in the derivative space-group (and which is not the identity representation in the supergroup: Salje 1985). The derivative space-group is called an *isotropy subgroup*, and the operations of the isotropy subgroup leave the distortion invariant.

In the *Ccmm* → *C2/m* transition, the translational symmetry remains unchanged, and the critical point of the Brillouin zone is the origin. Thus the primary order-parameter must transform under a Γ point (zone-center) representation of *Ccmm*. Stokes & Hatch (1988) considered the symmetry aspects of such transitions. Inspection of their Table 1 shows that the active order-parameter must transform according to the one-dimensional representation Γ_3^+ of *Ccmm*. This is a pure ferroelastic transition (Aizu 1969), and both Landau and Lifshitz frequencies are zero, as required for a continuous transition. As this is a proper ferroelastic transition, the basis functions of the irreducible representation transform as the components of the spontaneous strain. Generalized strain-tensor components are given by Schlenker *et al.* (1978). For the staurolite transition *Ccmm* → *C2/m*, and in terms of the underlying Cartesian axes $x//a_o$, $y//b_o$, $z//c_o$, the (Lagrangian) component(s) of the spontaneous strain is

$$x_5 = 1/2(a/a_o \cos\beta) \qquad (6)$$

where the subscript denotes the parameter(s) in the orthorhombic structure and the unsubscripted parameters correspond to the monoclinic structure. As the strain components transform as the order parameter for the representation Γ_3^+, the spontaneous strain could drive the transition and function as the principal order-parameter. The cell parameters for the orthorhombic case in the above expression are the values that the orthorhombic structure would have if it were stable under the conditions of stability of the monoclinic structure. Inspection of the cell dimensions of the refined structures of staurolite shows that for a specific composition (bulk sample), the cell dimensions *a, b, c* and *V* remain essentially constant, whereas the β angle can vary significantly. Specific examples are given in Table 2. This feature is particularly marked for samples 71–62R [crystals S(1–3)] and 117189 [crystals S(11–14)], the latter spanning a range in β from 90.03 to 90.45° without significant change in any of the other cell parameters [note that in principle, *a, b, c* and *V* cannot all remain constant with varying β angle, as β affects the cell volume; however, as $\beta \approx 90°$, sinβ does not change significantly (with respect to the precision of measurement) in the range of the observed β angle]. Thus in the above expression, $a_o \approx a$, and the active component of the spontaneous strain becomes 1/2 cosβ.

It is apparent from Figures 1–7 that there are many possible choices for the primary order-parameter. Each of these order parameters will couple bilinearly

TABLE 2. CELL DIMENSIONS[1] OF SELECTED STAUROLITE CRYSTALS FROM HAWTHORNE *ET AL.* (1993a)

Crystal	S(1)	S(2)	S(3)	S(11)	S(12)	S(13)	S(14)
a(Å)	7.863	7.863	7.865	7.868	7.868	7.868	7.869
b	16.613	16.612	16.608	16.610	16.609	16.609	16.606
c	5.650	5.650	5.651	5.658	5.658	5.659	5.659
β(°)	90.09	90.14	90.23	90.03	90.13	90.27	90.45
V(Å³)	738.1	738.1	738.1	739.5	739.4	739.6	739.5

[1] standard deviations are < 0.002 Å for *a* and *c*, < 0.004 Å for *b* and < 0.02° for *β*.

to the primary order-parameter, and hence affect the free energy. The primary order-parameter is that parameter that drives the transition. In the absence of a method to calculate the relative contributions of each order-parameter to the free energy, the selection of the primary order-parameter is somewhat arbitrary, and relies on intuition rather than a quantitative comparison of the energetics of the different structural parameters.

Symmetry-breaking displacements of coordinates

Let us consider the principal shifts in coordinates associated with the transition (*i.e.*, those that transform as the active irreducible representation of *Ccmm*). All trends are linear (Figs. 6, 7), and [except for the x parameter of O(4)] pass through the points $\delta x,y,z = 0$, $\beta = 90°$. There is some effect of composition on these relationships. For the O(1*A*)–O(1*B*) pair, the δx trend shows significant compositional effects, with the hydrogen-rich staurolite S(1–3) and Zn-rich staurolite S(11–14) showing larger and smaller slopes, respectively, than the general trend; in addition, the Mg-rich staurolite S(41) shows a completely different behavior, with a large negative δx value for $\beta \approx 90°$ (Fig. 6). Similar deviations are shown by some of the other parameters as well, but the effects are less pronounced. For the moment, we shall ignore these minor perturbations and focus on the principal trends.

As indicated in Figures 6 and 7, there are two types of displacement that can occur: (1) differences between analogous coordinates of pseudosymmetrically related pairs of atoms (Fig. 6), and (2) displacements from special positions of the higher-symmetry structure (Fig. 7). As is apparent from inspection of Figures 6 and 7, some displacements are far more pronounced than others, and hence are presumably more important from an energetic viewpoint. The larger displacements occur for both x and z of the O(1*A*) – O(1*B*) pair, and the z coordinates of O(3), *T*(1), *T*(2) and *M*(2). Displacements for O(4) and O(5) are small. Note that O(1*A*), O(1*B*) and O(3) are bonded to species at the *M*(3*A*), *M*(3*B*), *M*(4*A*), *M*(4*B*) and *T*(2) sites; these are all cation sites that are involved in extensive order–disorder, and their coordination polyhedra all share corners, edges and faces. The origin of the unit cell occurs at the *M*(3*A*) site, and both *M*(3*A*) and *M*(3*B*) lie on the *c* axis. As indicated above, in the orthorhombic structure, there is a mirror plane perpendicular to *c* and passing through the edge shared between the *M*(3*A*) and *M*(3*B*) octahedra. In the transition *Ccmm* → *C2/m*, this mirror plane is lost and (as shown by the data), the β angle departs from 90°. This change in the β angle actually shears the original orthorhombic structure in the manner indicated in Figure 2b. Such a shear must change the interatomic angles but need not necessarily change the (nearest-neighbor) cation–anion distances significantly. Cation–anion distances can change for two reasons: (1) there is a direct local change in the site occupancies, such as the substitution □ ⇌ Al or Mg ⇌ Al; (2) there is a change induced by site-occupancy changes at next-nearest-neighbor sites (commonly called an inductive effect). The first process involves a primary change in the local stereochemistry, whereas the second process occurs in response to the first process occurring at a next-nearest-neighbor site. It is important to recognize which atomic displacements involve which process, because the primary order-parameter (and important secondary order-parameters) should involve displacements of the first sort, resulting directly from a local stereochemical rearrangement (note that this argument is made specifically for the transition in staurolite, and is not necessarily relevant to other transitions of this sort). This argument is in line with the pattern of displacements observed in staurolite (Figs. 6, 7).

For the anions, the principal shifts in coordinates affect O(1*A*), O(1*B*) and O(3), anions that constitute the coordination polyhedra of the *M*(3*A*) and *M*(3*B*) sites that are involved in the most extensive order–disorder of the series. Thus it seems reasonable to suppose that these shifts occur as a result of the constituent order–disorder, and in support of this, the variations in mean bond-lengths at these two sites are in line with this conclusion.

On the other hand, the O(2) and O(4) anions show much smaller variations in their displacements. These anions are involved in the coordination polyhedra around the *T*(1), *M*(1*A*), *M*(1*B*) and *M*(2) sites that are not involved in extensive order–disorder of cations, although there is the possibility of limited Mg–Al order over the *M*(1*A*) and *M*(1*B*) sites.

For the cations, the principal shifts in coordinates occur for the z parameters of *T*(1), *T*(2) and *M*(2), with the displacements for *T*(2) being approximately twice those of *T*(1) and *M*(2). The shear induced in the structure by the change in β angle will move these three sites in the directions indicated by their displacements. Thus it seems reasonable to assume that these shifts occur directly as a result of the spontaneous strain. However, there may be an additional contribution for the *T*(2) site. There is significant positional disorder of the cations occupying *T*(2) (Smith 1968, Alexander 1989). Although it is not possible to assign accurate occupancies to the three constituent subsites (because their separation is less than half the wavelength of the scattered radiation), the trends seen by Hawthorne *et al.* (1993a) indicate that the subsite ordering is a function of the β angle, with the *T*(2*b*) site (with the smallest z coordinate) showing increased occupancy with increasing β. Thus with increasing order over the *T*(2) subsites, the z coordinate of the aggregate electron density will decrease. This decrease occurs in addition to the displacement induced by the spontaneous strain, and accounts for the fact that the shift in the z coordi-

nate of $T(2)$ is much larger than the shifts in the z coordinates of $T(1)$ and $M(2)$.

In conclusion, the principal displacements are associated with the atoms locally involved in cation order–disorder, with additional displacements arising from the structural shear associated with the spontaneous strain. Thus it seems reasonable to take an order parameter involving one of the cations as the principal order-parameter.

Symmetry-preserving coordinate-displacements

Inspection of the positional coordinates of the refined structures of staurolite shows that there are changes in coordinates that do not transform as the active irreducible representation of the transition. Table 1 shows that these involve the x and y coordinates of O(3), O(5), $T(1)$ and $M(2)$, and the x coordinate of $T(2)$. Also involved are the average coordinates of the A–B pairs of atoms. The magnitudes of the variations of these coordinates are generally small (< 0.0020); they show no significant correlation with the β angle, but do correlate with differences in composition.

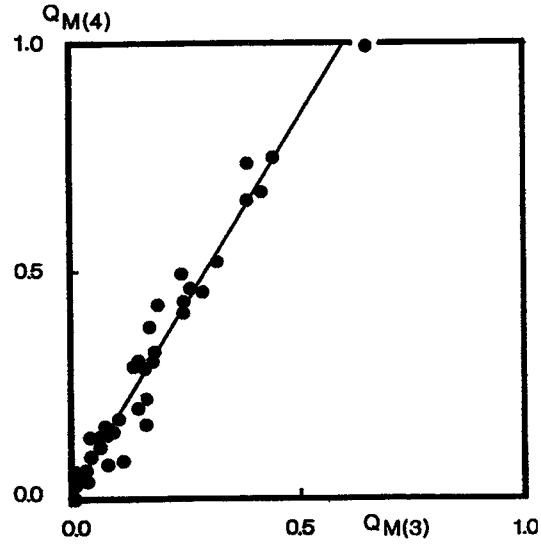

FIG. 8. Variation in order parameters involving distribution of Al and □ over $M(3A)$–$M(3B)$ and distribution of (Fe, Mg...) and □ over $M(4A)$–$M(4B)$.

Cation order–disorder

There are three distinct cation-ordering processes in staurolite: (1) Al – □ over $M(3A)$–$M(3B)$; (2) (Fe,Mg) – □ over $M(4A)$–$M(4B)$; (3) (Fe,Zn...) – □ over $T(2a)$–$T(2b)$–$T(2c)$; in addition, there may be some Mg–Al order–disorder over $M(1A)$–$M(1B)$. It is now necessary to decide which of these is energetically dominant. A reasonable starting point is to assume that the process involving the largest local stereochemical differences is the most important from an energetic viewpoint. Bond-valence considerations (Hawthorne *et al.* 1993b) indicate that cation – □ ordering is much more structurally perturbing that cation–cation ordering; thus we do not consider Mg–Al ordering at $M(1A)$–$M(1B)$ any further. The (Fe...) – □ ordering over the $T(2)$ subsites is primarily a positional disorder off a central $T(2)$ site. This disorder does not leave a vacancy in this cavity as a whole (unless the presence of vacancies is implicit in the bulk composition), but simply readjusts the local bond-valence distribution; Hawthorne *et al.* (1993b) show that this occurs as a result of cation – □ ordering at other sites in the structure. Hence we are left with the cation – □ processes involving $M(3A)$–$M(3B)$ and $M(4A)$–$M(4B)$. The correlation between the corresponding two order-parameters is shown in Figure 8; it is linear, but the slope is not unity. Thus although the β angle is linear with the order parameter for the $M(4A)$–$M(4B)$ sites, β seems to increase after the $M(4A)$–$M(4B)$ order-parameter reaches its limiting value of unity. Consequently, this is unlikely to be the primary order-parameter, otherwise this further increase in β would not be expected. In addition, the very small site-populations normally observed for $M(4A)$ and $M(4B)$ suggest that this will not be the energetically dominant process. This leaves Al – □ ordering over $M(3A)$–$M(3B)$ as the remaining candidate for the primary order-parameter. This seems the best choice from every viewpoint. The sites are on average half occupied, allowing a completely ordered structure to exist at the maximum value of β. The local difference between occupancy by Al (charge = 3+) and □ (charge = 0) is extreme, and must cause significant differences in energy (and also other changes in local order: see Hawthorne *et al.* 1993b).

Thus Al–□ ordering over $M(3A)$–$M(3B)$ is the primary order-parameter. Other order-parameters couple to this structurally *via* the local bond-valence requirements of the anions. Atomic positions all displace, again to satisfy local bond-valence requirements, and these positional displacements all couple to the spontaneous strain. Hence we have a detailed and physically reasonable microscopic model for the $Ccmm \rightarrow C2/m$ transition in staurolite.

SUMMARY

1. At room temperature, staurolite is monoclinic, $C2/m$, with observed β varying in the range 90–90.45°.

2. The monoclinic $C2/m$ structure is pseudo-orthorhombic, with the ideal space-group $Ccmm$.

3. *C2/m* is an isotropy subgroup of *Ccmm*, suggesting the possibility of a second-order phase transition, both Landau and Lifshitz frequencies being zero; this is a pure ferroelastic transition.
4. All ordering processes in staurolite transform as the active irreducible representation of the *Ccmm* → *C2/m* transition, and the associated order-parameters are linear with varying β angle (*i.e.*, they are coupled to the spontaneous strain).
5. All coordinate shifts that transform as the active irreducible representation of the transition are linear functions of the spontaneous strain.
6. These parameter shifts (both coordinates and ordering parameters) extrapolate to zero at β = 90° with one significant exception: the *x* coordinate of the O(4) anion is displaced ~0.15 Å from its ideal special position in the *Ccmm* structure.
7. At room temperature, all parameters of the staurolite structure with β = 90° obey orthorhombic *Ccmm* symmetry *except* the *x* coordinate of the O(4) anion. Thus staurolite is monoclinic at room temperature.
8. It is a reasonable surmise that staurolite becomes truly orthorhombic at higher temperatures.
9. If the *x* coordinate of O(4) goes continuously to zero with increasing temperature, the transition is completely second order; if the *x* coordinate of O(4) goes discontinuously to zero, the transition will have a small amount of first-order character.
10. Detailed examination of the active atomic displacements shows that they can all be associated with a structural shear that is the spontaneous strain (= cosβ) associated with the transition. These displacements are also associated with the principal cation-ordering processes over the *M*(3*A*)–*M*(3*B*), *M*(4*A*)–*M*(4*B*) and *T*(2) sites.
11. The primary order-parameter of the transition is Al – □ ordering over the *M*(3*A*)–*M*(3*B*) sites.
12. Staurolite can be represented as an order–disorder series between a completely ordered monoclinic end-member (*C2/m*, β = 90.64°, *M*(3*A*) = Al, *M*(3*B*) = □) and a completely disordered orthorhombic end-member (*Ccmm*, β = 90°, *M*(3*A*) = *M*(3*B*) = 0.5 Al + 0.5 □).

Acknowledgements

We thank the referees for their comments that "tightened up" the paper considerably. Financial support was provided by the Natural Sciences and Engineering Research Council of Canada and the CNR Centro di Studio per la Cristallochimica e la Cristallografia, Pavia.

References

Aizu, K. (1969): Possible species of "ferroelastic" crystals and of simultaneously ferroelectric and ferroelastic crystals. *J. Phys. Soc. Jap.* **27**, 387-396.

Alexander, V.D. (1989): Iron distribution in staurolite at room and low temperatures. *Am. Mineral.* **74**, 610-619.

Bringhurst, K.N. & Griffen, D.T. (1986): Staurolite – lusakite series. II. Crystal structure and optical properties of a cobaltoan staurolite. *Am. Mineral.* **71**, 1466-1472.

Carpenter, M.A., Domeneghetti, M.-C. & Tazzoli, V. (1990a): Application of Landau theory to cation ordering in omphacite. I. Equilibrium behaviour. *Eur. J. Mineral.* **2**, 7-18.

———, ——— & ——— (1990b): Application of Landau theory to cation ordering in omphacite. II. Kinetic behaviour. *Eur. J. Mineral.* **2**, 19-28.

Ghose, S., Ito, Y. & Hatch, D.M. (1991): Paraelectric – antiferroelectric phase transition in titanite, $CaTiSiO_5$. I. A high temperature x-ray diffraction study of the order parameter and transition mechanism. *Phys. Chem. Miner.* **17**, 591-603.

Hanisch, K. (1966): Zur Kenntnis der Kristallstrucktur von Staurolith. *Neues Jahrb. Mineral. Monatsh.*, 362-366.

Hatch, D.M., Artman, J.I. & Boerio-Goates, J. (1990a): Phase transition in $K_2Cd_2(SO_4)_3$: order parameter and microscopic distortions. *Phys. Chem. Miner.* **17**, 334-343.

———, Ghose, S. & Stokes, H.T. (1990b): Phase trasitions in leucite, $KAlSi_2O_6$. I. Symmetry analysis with order parameter treatment and the resulting microscopic distortions. *Phys. Chem. Miner.* **17**, 220-227.

——— & Griffen, D.T. (1989): Phase transitions in the grandite garnets. *Am. Mineral.* **74**, 151-159.

———, Stokes, H.T. & Putnam, R.M. (1987): Symmetry analysis of the microstructure and phase transitions of a crystallographic space group: applications. *Phys. Rev.* **B35**, 4935-4942.

Hawthorne, F.C., Ungaretti, L., Oberti, R., Caucia, F. & Callegari, A. (1993a): The crystal chemistry of staurolite. I. Crystal structure and site occupancies. *Can. Mineral.* **31**, 551-582.

———, ———, ———, ——— & ——— (1993b): The crystal chemistry of staurolite. III. Local order and chemical composition. *Can. Mineral.* **31**, 597-616.

Hurst, V.J., Donnay, J.D.H. & Donnay, G. (1956): Staurolite twinning. *Mineral. Mag.* **31**, 145-163.

Kocinsky, J. (1983): *Theory of Symmetry Changes at Continuous Phase Transitions.* Elsevier, New York.

Náray-Szabó, I. (1929): The structure of staurolite. *Z. Kristallogr.* **71**, 103-116.

——— & Sasvári, K. (1958): On the structure of staurolite $HFe_2Al_9Si_4O_{24}$. *Acta Crystallogr.* **11**, 862-865.

Ribbe, P.H. (1982): Staurolite. *In* Orthosilicates (P.H. Ribbe, ed.). *Rev. Mineral.* **5**, 171-188.

SALJE, E. (1985): Thermodynamics of sodium feldspar. I. Order parameter treatment and strain induced coupling effects. *Phys. Chem. Miner.* **12**, 93-98.

——— (1987): Structural states of Mg-cordierite. II. Landau theory. *Phys. Chem. Miner.* **14**, 455-460.

———, KUSCHOLKE, B., WRUCK, B. & KROLL, H. (1985): Thermodynamics of sodium feldspar. II. Experimental results and numerical calculations. *Phys. Chem. Miner.* **12**, 99-107.

SCHLENKER, J.L., GIBBS, G.V. & BOISEN, M.B., JR. (1978): Strain-tensor components expressed in terms of lattice parameters. *Acta Crystallogr.* **A34**, 52-54.

SHANNON, R.D. (1976): Revised effective ionic radii and systematic studies of interatomic distances in halides and chalcogenides. *Acta Crystallogr.* **A32**, 751-767.

SMITH, J.V. (1968): The crystal structure of staurolite. *Am. Mineral.* **53**, 1139-1155.

STÅHL, K., KVICK, Å. & SMITH, J.V. (1988): A neutron diffraction study of hydrogen positions at 13 K, domain model, and chemical composition of staurolite. *J. Sol. State Chem.* **73**, 362-380.

STOKES, H.T. & HATCH, D.M. (1988): *Isotropy Subgroups of the 230 Crystallographic Space Groups*. World Scientific, Singapore.

TAGAI, T. & JOSWIG, W. (1985): Unterschungen der Kationenverteilung im Staurolith durch Neutronenbeugung bei 100 K. *Neues Jahrb. Mineral. Monatsh.*, 97-107.

TOLÉDANO, J.-C. & TOLÉDANO, P. (1987): *The Landau Theory of Phase Transitions*. World Scientific, Singapore.

Received May 26, 1992, revised manuscript accepted November 5, 1992.